Supporting information

High capacity and fast Na^+ transportation in $SbPS_4$ material by Bi^{3+} substitution for sodium-ion batteries

Qi-Min Yin[a+], Zhen-Yi Gu[b+], Hong-Yan Lü[a], Weiping Guo[c], Miao Du[a], Yi-Tong Liu[a], Yan Liu[a], Yong-Li Heng[b], Zhong-Zhen Luo*[c], and Xing-Long Wu*[a,b]*

[a] *Department of Chemistry, Northeast Normal University, Changchun, Jilin 130024, P. R. China*

[b] *MOE Key Laboratory for UV Light-Emitting Materials and Technology, Northeast Normal University, Ministry of Education, Changchun, Jilin 130024, P. R. China*

[c] *Key Laboratory of Eco-materials Advanced Technology, College of Materials Science and Engineering, Fuzhou University, Fuzhou, 350108, P. R. China*

+ Q.-M. Yin and Z.-Y. Gu contributed equally.

Contents in the Supporting Information

1. Materials Preparation 4

1.1 Synthesis of $Sb_{1-x}Bi_xPS_4$ anode materials 4

1.2 Synthesis of $Na_3V_2(PO_4)_2O_2F$ cathode materials 4

1.3 Material Characterization 5

1.4 Electrochemical Measurements 5

2. Results and discussion 7

2.1 *Structural Characterization of $Sb_{0.7}Bi_{0.3}PS_4$* 7

Figure S1. SEM of $Sb_{1-x}Bi_xPS_4$ (a) $SbPS_4$ (b) $Sb_{0.9}Bi_{0.1}PS_4$ (c) $Sb_{0.8}Bi_{0.2}PS_4$ and (d) $Sb_{0.6}Bi_{0.4}PS_4$. 7

2.2 *Electrochemical Performance of $Sb_{1-x}Bi_xPS_4$* 8

Figure S2. Long cycles of $Sb_{0.7}Bi_{0.3}PS_4$ and $Sb_{0.6}Bi_{0.4}PS_4$ in half cells at 1 A g^{-1} 8

Figure S3. Galvanostatic curves of $Sb_{0.7}Bi_{0.3}PS_4$ in half cells at 1 A g^{-1}. 8

Figure S4. EIS tests for $Sb_{1-x}Bi_xPS_4$. 9

2.3 *Kinetics Analysis of $Sb_{0.7}Bi_{0.3}PS_4$* 9

Figure S5. $SbPS_4$ material of (a) CV curves at different scan rates, (b) Normalized contribution ratio of capacitive and diffusion-controlled capacities. 9

Figure S6. $Sb_{0.9}Bi_{0.1}PS_4$ material of (a) CV curves at different scan rates, (b) Normalized contribution ratio of capacitive and diffusion-controlled capacities. 10

Figure S7. $Sb_{0.8}Bi_{0.2}PS_4$ material of (a) CV curves at different scan rates, (b) Normalized contribution ratio of capacitive and diffusion-controlled capacities. 10

Figure S8. $Sb_{0.6}Bi_{0.4}PS_4$ material of (a) CV curves at different scan rates, (b) Normalized contribution ratio of capacitive and diffusion-controlled capacities. 11

2.4 *Full cell Application* 11

Figure S9. XRD of $Na_3V_2(PO_4)_2O_2F$ materials. 11

Figure S10. SEM of $Na_3V_2(PO_4)_2O_2F$ materials. 12

Figure S11. Electrochemical properties of $Na_3V_2(PO_4)_2O_2F$ in half cells:(a) Rate capabilities from 0.1 C to 5 C and (b) the corresponding galvanostatic curves. 12

Figure S12. Practical demonstrations of coin-type full battery for lighting LED bulbs. 13

Table S1 Comparison of $Sb_{0.7}Bi_{0.3}PS_4$ materials from our work with previously reported ones of anode materials for sodium ion batteries. 13

References 13

Experimental section

1. Materials Preparation

All of the chemical reagents were purchased from Aladdin and used as received without any purification.

1.1 Synthesis of $Sb_{1-x}Bi_xPS_4$ anode materials

The $Sb_{1-x}Bi_xPS_4$ anode materials were prepared according to the previous report.[1] The corresponding stoichiometric ratio of Sb, Bi, P and S for $Sb_{1-x}Bi_xPS_4$ are added into the molten silicon tube and sealed under vacuum (<10^{-4} Torr). The mixture rises to 200 ℃ for 4 hours, then rises to 650 ℃ for 48 hours, and then cools to 50 ℃ at 12 ℃/min.

1.2 Synthesis of $Na_3V_2(PO_4)_2O_2F$ cathode materials

The $Na_3V_2(PO_4)_2O_2F$ cathode materials were prepared via a simple hydrothermal method according to our recent report.[2] Briefly, V_2O_5 and $H_2C_2O_4$ with the molar ratio of 1:3 were dissolved in the distilled water under stirring at 70 ℃ for 1 hour. And then, stoichiometric $NH_4H_2PO_4$ and NaF were added into the above-formed transparent solution under continuous stirring. After the pH of the solution was adjusted to the required value of 7 by using ammonium hydroxide, the obtained solution was transferred into a Teflon-lined autoclave and heated at the setting temperature of 170 ℃ for 12 hours followed by a natural cooling outside the oven to room temperature. Finally, the $Na_3V_2(PO_4)_2O_2F$ products could be easily collected after washing the precipitation with distilled water and ethanol several times, and then drying in a vacuum at 80 ℃.

1.3 Material Characterization

The XRD patterns of $Sb_{1-x}Bi_xPS_4$ and $Na_3V_2(PO_4)_2O_2F$ were performed by X-ray powder diffractometer (XRD, Bruker D8) with Cu Kα at λ = 0.15406 nm to investigate the phase composition. The elemental composition and valence states of $Sb_{0.7}Bi_{0.3}PS_4$ were characterized by the X-ray photoelectron spectrum (XPS, Thermo). The morphology features of $Sb_{1-x}Bi_xPS_4$ were tested by transmission electron microscopy (TEM, JEOL-2100F) and scanning electron microscopy (SEM, Hitachi-SU8000). The distribution of elements for $Sb_{0.7}Bi_{0.3}PS_4$ was observed by energy-dispersive X-ray spectroscopy (EDS).

1.4 Electrochemical Measurements

The CR2032-type coin cells were assembled in the argon-filled glove at an atmosphere that is H_2O and O_2 lower than 0.1 ppm. The electrolyte was composed of 1.0 M $NaClO_4$ in propylene carbonate with 5% fluoroethylene carbonate. The glass fibrous membrane was used as the separator. The sodium metal was used as the reference and counter electrode in the half cell. The electrode of $Sb_{1-x}Bi_xPS_4$ was composed of 70 wt.% active materials, 20 wt.% carbon black and 10 wt.% sodium alginate mixed with DI water on Cu foil, then dried in a vacuum oven at 60 °C overnight.

The average mass loading of $Sb_{1-x}Bi_xPS_4$ material is about 1 mg cm^{-2} in the half/full sodium ion batteries. The range voltage of $Sb_{1-x}Bi_xPS_4$ was 0.05-2 V *vs*. Na^+/Na tested by LAND CT2001A. The cyclic voltammetry (CV) was performed on the CHI 750 electrochemical workstation of ChenHua. The Electrochemical Impedance Spectroscopy of $Sb_{0.7}Bi_{0.3}PS_4$ material was carried out on Solartron Frequency Response

Analyzer 1260A under the frequency of 100 kHz to 1 Hz.The Electrochemical Impedance Spectroscopy of $Sb_{1-x}Bi_xPS_4$ material was carried out on CHI 750 under the frequency of 100 kHz to 0.1 Hz. For full battery assembly, the $Na_3V_2(PO_4)_2O_2F$ and $Sb_{0.7}Bi_{0.3}PS_4$ materials were used as cathode and anode, respectively. The electrochemical performance of $Na_3V_2(PO_4)_2O_2F$ was tested at the potential of 2.0 – 4.5 V *vs*. Na^+/Na in the half cell. The full battery of $Na_3V_2(PO_4)_2O_2F$ //$Sb_{0.7}Bi_{0.3}PS_4$ was tested on the voltage range of 1-3.5 V. The electrode of $Na_3V_2(PO_4)_2O_2F$ was composed of active materials, carbon black and sodium alginate mixed with DI water in a mass ratio of 7:2:1 sodiated chemically before assembling the full cell. The mass ratio of cathode and anode was 2:1 for the full cell tests. Before the assembly of the full cell, all $Sb_{0.7}Bi_{0.3}PS_4$ anodes were subjected to electrochemical pre-sodiation. In pre-sodiation specific process, the $Sb_{0.7}Bi_{0.3}PS_4$ anodes cycled 4 times at 0.2 A g^{-1}.

The relationship between the peak current *i* and scan rate *v* can be described as the following formulas:

$$i = av^b$$

$$\log(i)=b\log(v)+\log(a)$$

The a is a constant, and b is the slope of log(*i*) versus log(*n*) plots. The b value approximates 0.5 representing a more diffusion-controlled behavior. While the value of b approaches 1, the electrochemical process contributes to capacitive-controlled behavior.

The capacitance contribution at a certain scan rate can be calculated by using the following formulas:

$$i = k_1 v + k_2 v^{1/2}$$

Herein, the $k_1 v$ and $k_2 v^{1/2}$ represent the capacitive contribution and diffusion-controlled contribution, respectively.

2. Results and discussion

2.1 *Structural Characterization of $Sb_{0.7}Bi_{0.3}PS_4$*

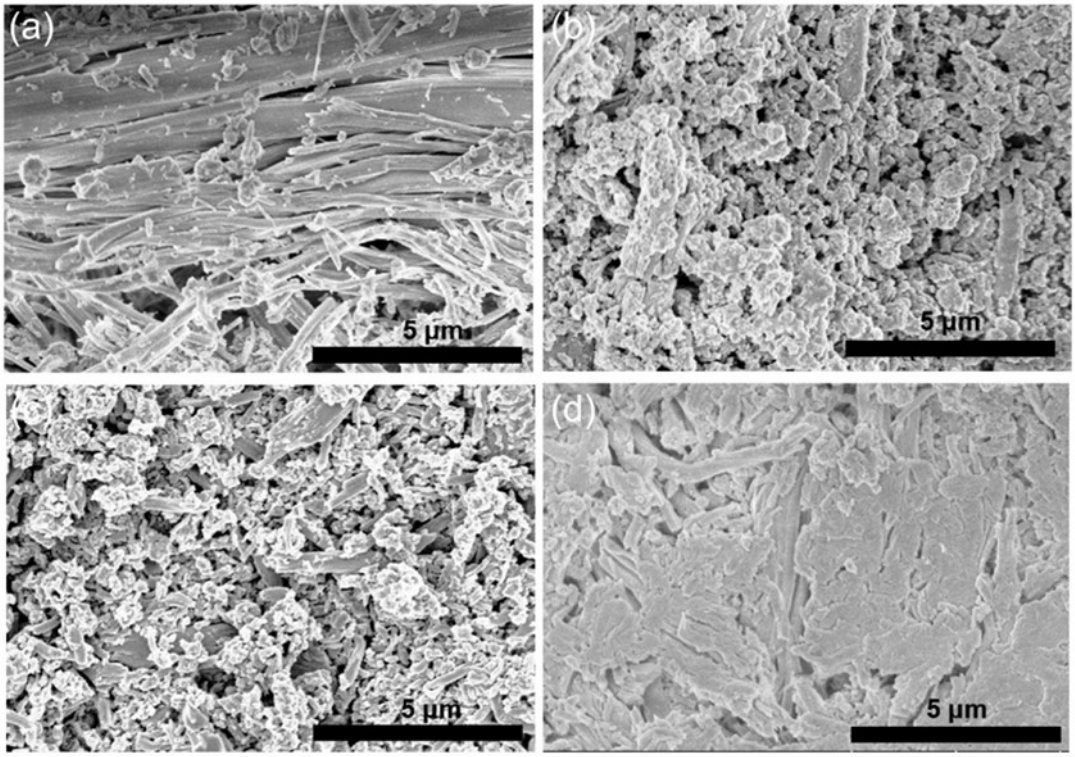

Figure S1. SEM of $Sb_{1-x}Bi_xPS_4$ (a) $SbPS_4$ (b) $Sb_{0.9}Bi_{0.1}PS_4$ (c) $Sb_{0.8}Bi_{0.2}PS_4$ and (d) $Sb_{0.6}Bi_{0.4}PS_4$.

2.2 *Electrochemical Performance of $Sb_{1-x}Bi_xPS_4$*

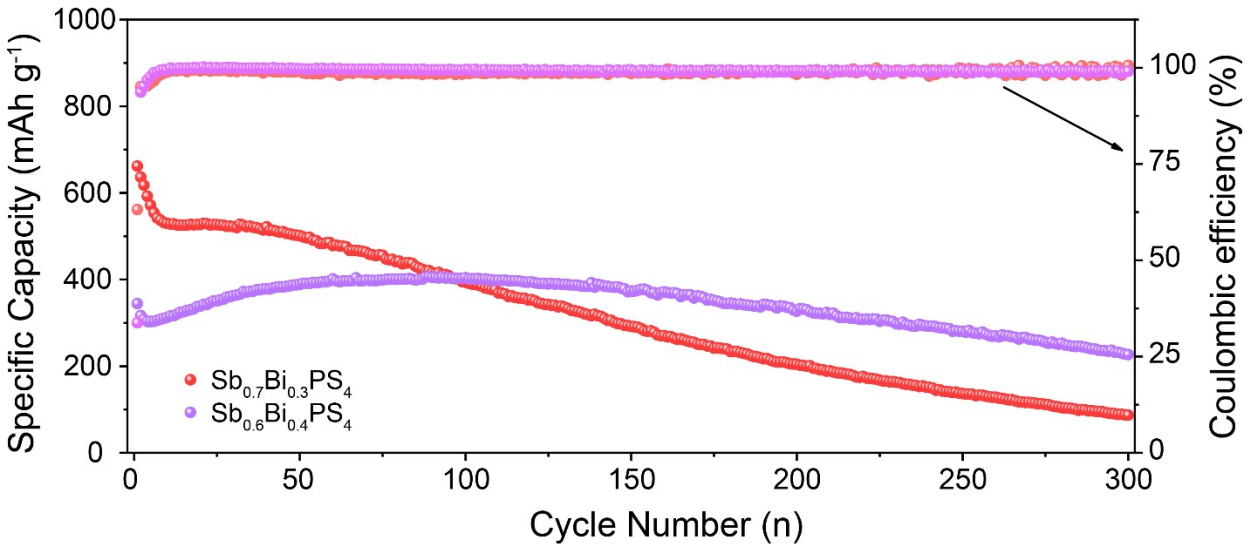

Figure S2. Long cycles of $Sb_{0.7}Bi_{0.3}PS_4$ and $Sb_{0.6}Bi_{0.4}PS_4$ in half cells at 1 A g^{-1}

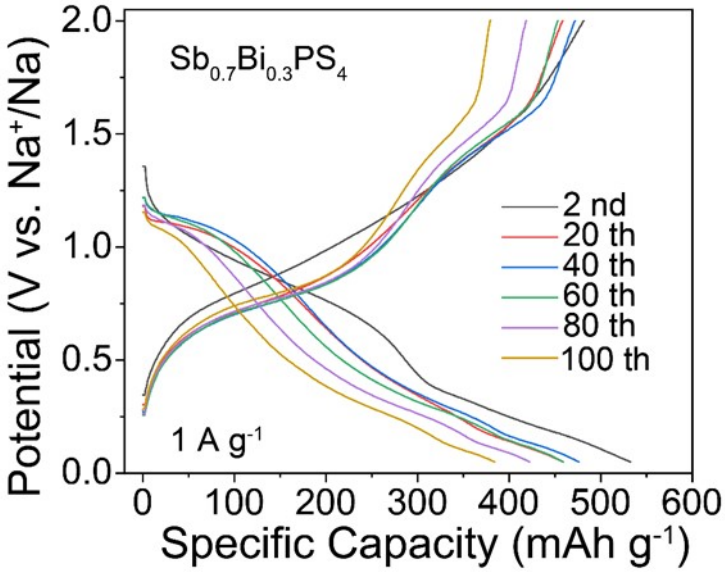

Figure S3. Galvanostatic curves of $Sb_{0.7}Bi_{0.3}PS_4$ in half cells at 1 A g^{-1}.

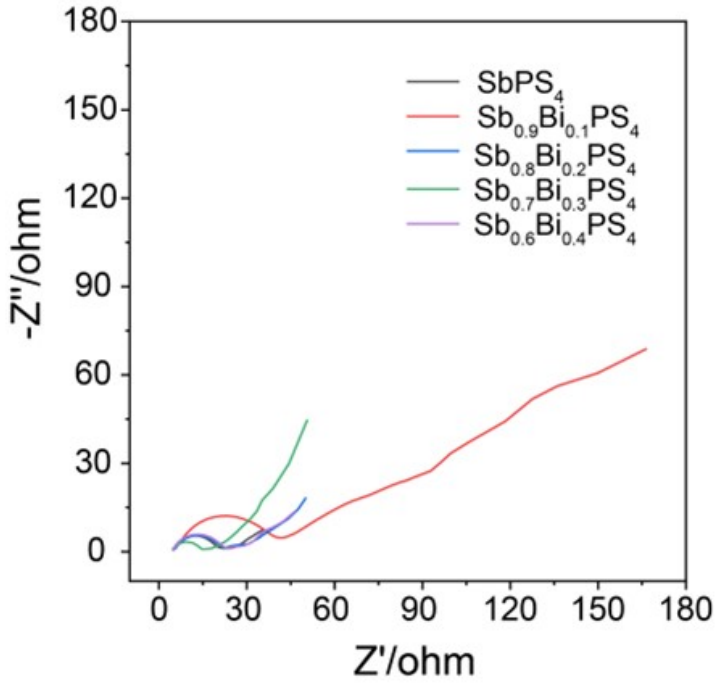

Figure S4. EIS tests for $Sb_{1-x}Bi_xPS_4$.

2.3 *Kinetics Analysis of $Sb_{0.7}Bi_{0.3}PS_4$*

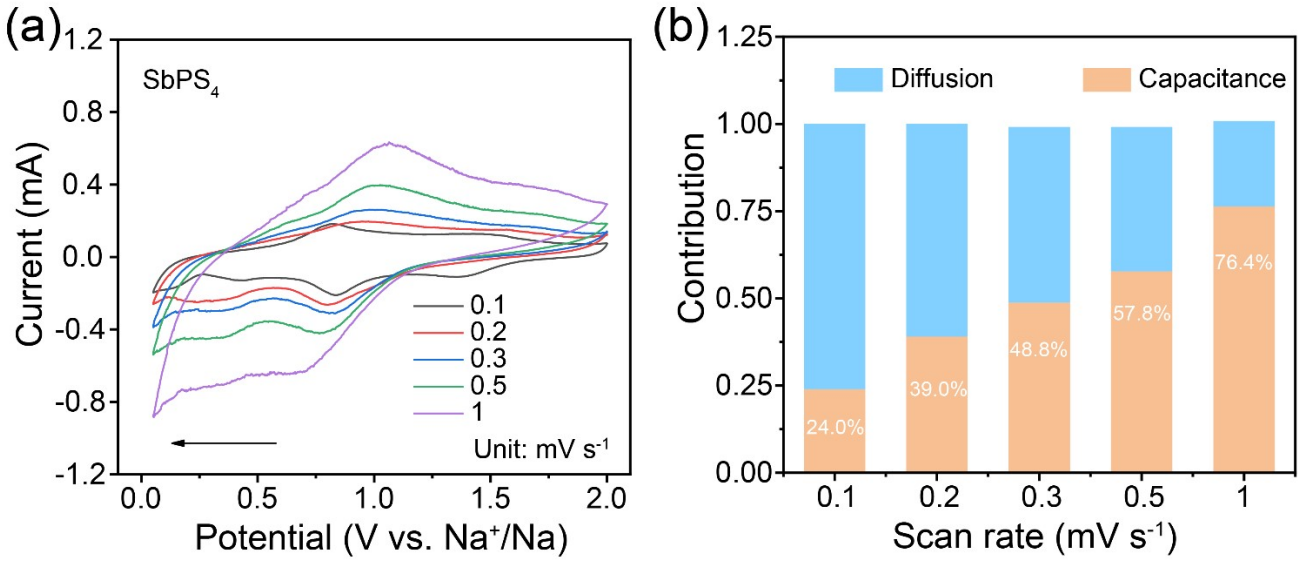

Figure S5. $SbPS_4$ material of (a) CV curves at different scan rates, (b) Normalized contribution ratio of capacitive and diffusion-controlled capacities.

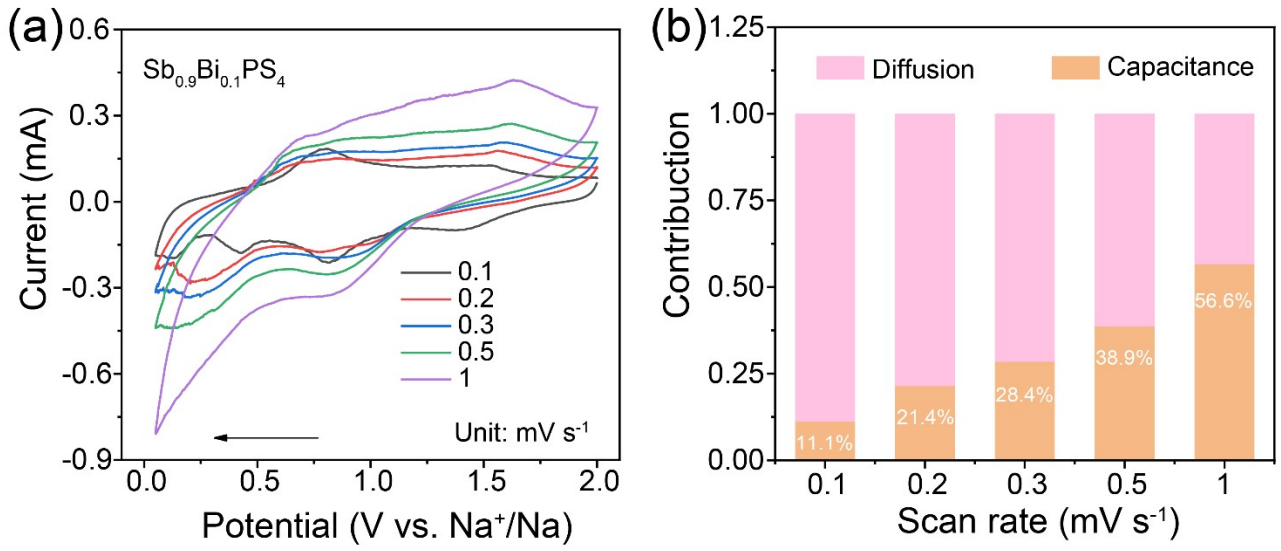

Figure S6. $Sb_{0.9}Bi_{0.1}PS_4$ material of (a) CV curves at different scan rates, (b) Normalized contribution ratio of capacitive and diffusion-controlled capacities.

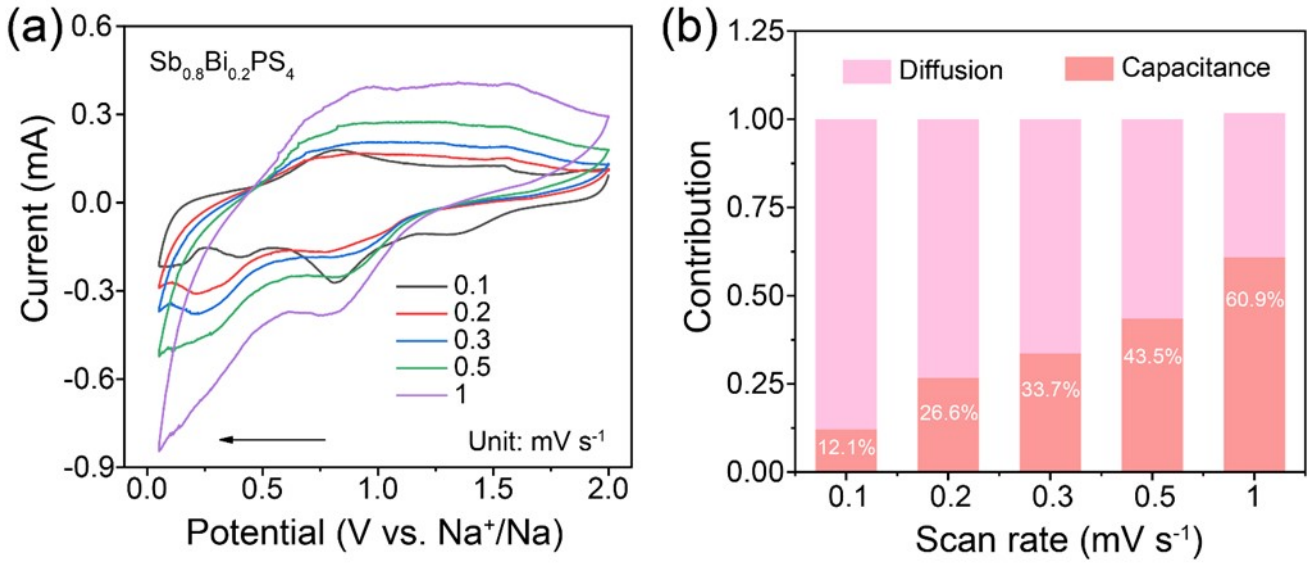

Figure S7. $Sb_{0.8}Bi_{0.2}PS_4$ material of (a) CV curves at different scan rates, (b) Normalized contribution ratio of capacitive and diffusion-controlled capacities.

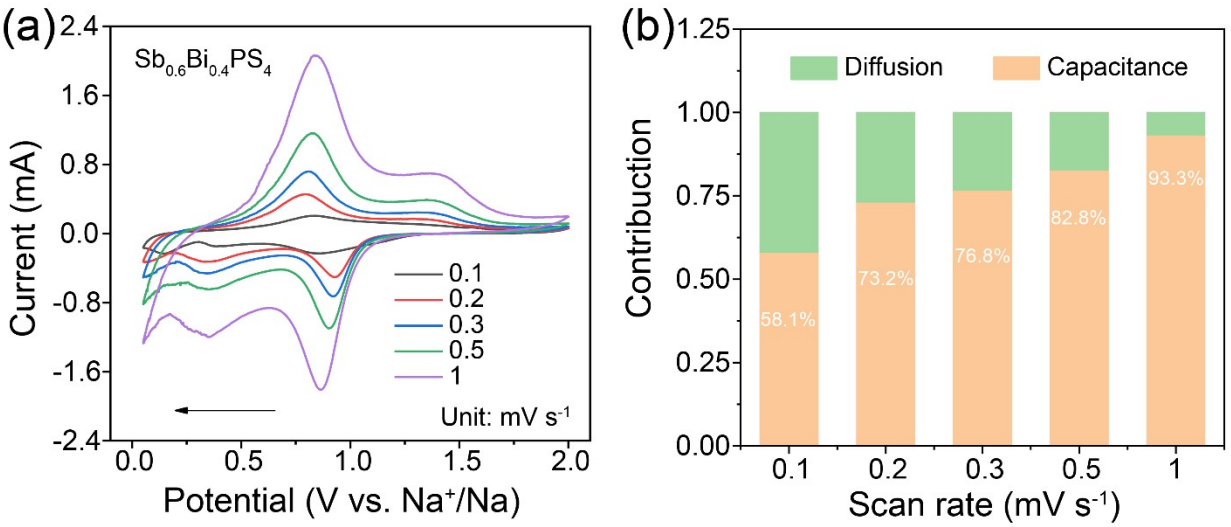

Figure S8. $Sb_{0.6}Bi_{0.4}PS_4$ material of (a) CV curves at different scan rates, (b) Normalized contribution ratio of capacitive and diffusion-controlled capacities.

2.4 *Full cell Application*

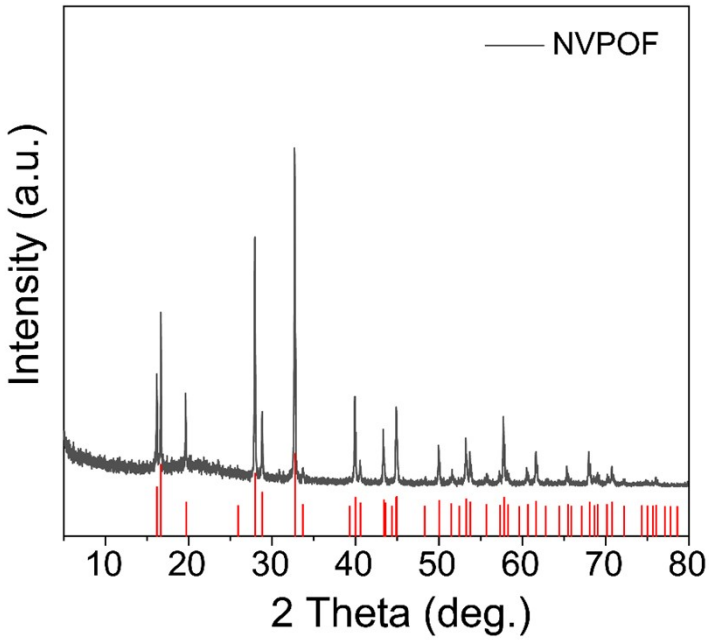

Figure S9. XRD of $Na_3V_2(PO_4)_2O_2F$ materials.

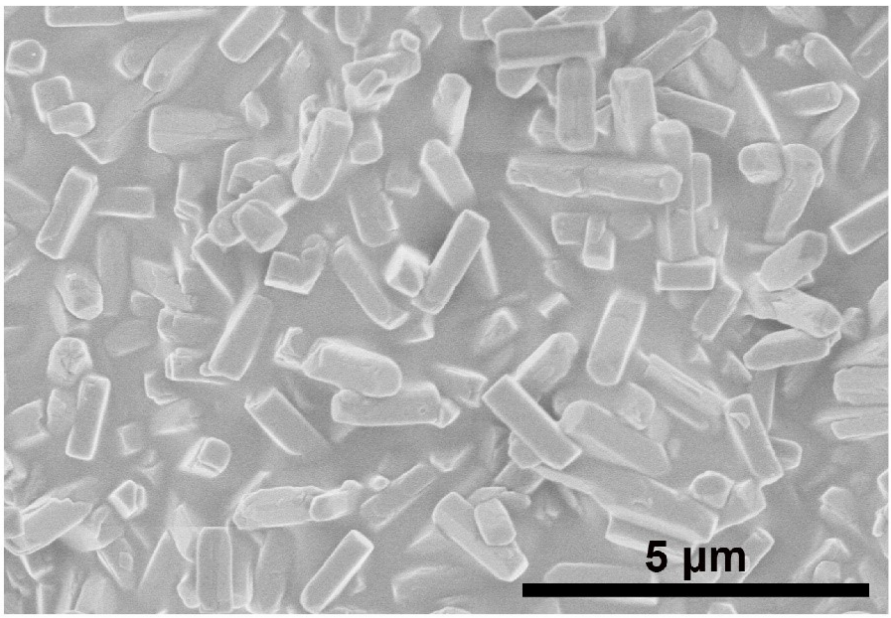

Figure S10. SEM of $Na_3V_2(PO_4)_2O_2F$ materials.

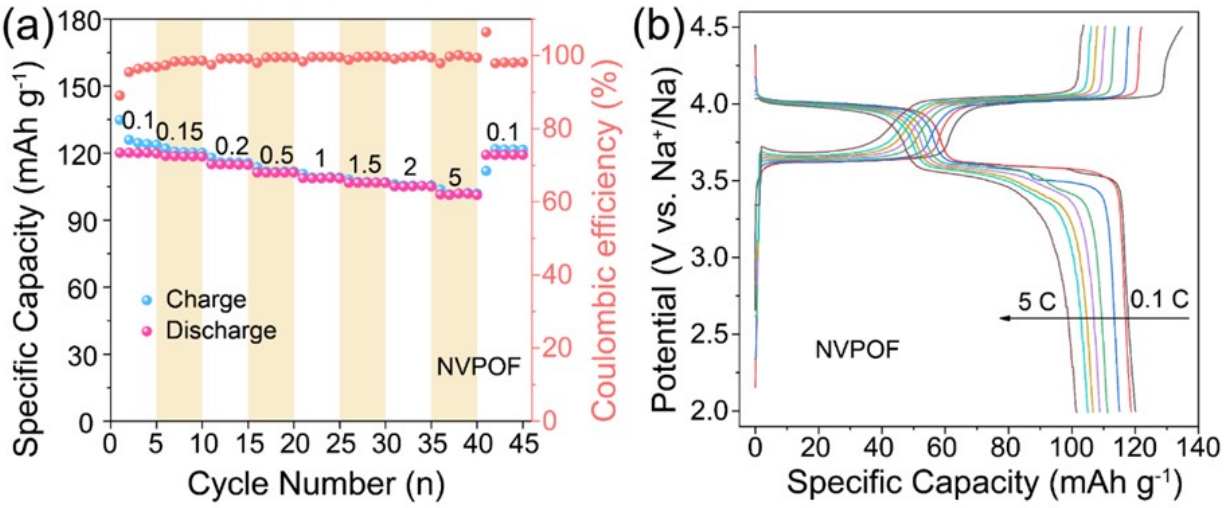

Figure S11. Electrochemical properties of $Na_3V_2(PO_4)_2O_2F$ in half cells:(a) Rate capabilities from 0.1 C to 5 C and (b) the corresponding galvanostatic curves.

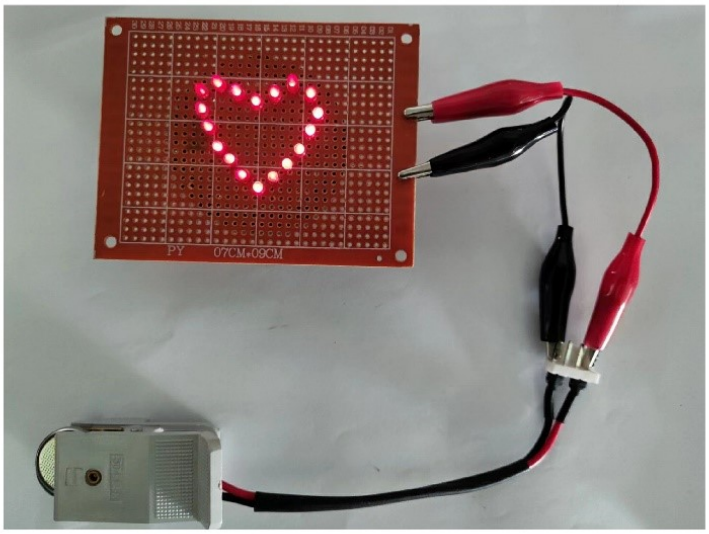

Figure S12. Practical demonstrations of coin-type full battery for lighting LED bulbs.

Table S1 Comparison of $Sb_{0.7}Bi_{0.3}PS_4$ materials from our work with previously reported ones of anode materials for sodium ion batteries.

Materials	Synthesis methods	Elctrochemical activity	Ref
$Sb_{0.7}Bi_{0.3}PS_4$	Annealing	831 mA h g^{-1} (0.1A g^{-1})	This work
FeP@OCF	Phosphorization	634 mA h g^{-1} (0.1A g^{-1})	[3]
$Sn_{4+x}P_3$@(Sn-P)	Ball milling	502 mA h g^{-1} (0.1 A g^{-1})	[4]
SnO_{2-x}/C	Electrospinning	650 mAh g-1 (0.1 A g^{-1})	[5]
Sb/C	Electrospinning	422 mA h g^{-1} (0.1 A g^{-1})	[6]
Bi@N−C	Solvothermal	478 mA h g^{-1} (0.05 A g^{-1})	[7]
Bi/rGO	Ball-milling	470 mA h g^{-1} (0.05 A g^{-1})	[8]
$BiPS_4$	Solvothermal	558 mA h g^{-1} (0.1 A g^{-1})	[9]
$MnPS_3$	Annealing	246 mA h g^{-1} (0.1A g^{-1})	[10]

References

1 C. D. Malliakas and M. G. Kanatzidis, *J. Am. Chem. Soc.*, 2006, **128**, 6538-6539.

2 J. Z. Guo, P. F. Wang, X. L. Wu, X. H. Zhang, Q. Yan, H. Chen, J. P. Zhang and Y. G. Guo, *Adv. Mater.*, 2017, **29**, 1701968.

3 S. Shi, C. Sun, X. Yin, L. Shen, Q. Shi, K. Zhao, Y. Zhao and J. Zhang, *Adv. Funct. Mater.*, 2020,

30, 1909283.

4 W. Li, S.-L. Chou, J.-Z. Wang, J. H. Kim, H.-K. Liu and S.-X. Dou, *Adv. Mater.*, 2014, **26**, 4037-4042.

5 D. Ma, Y. Li, H. Mi, S. Luo, P. Zhang, Z. Lin, J. Li and H. Zhang, *Angew. Chem. Int. Ed.*, 2018, **57**, 8901-8905.

6 Y. Yuan, S. Jan, Z. Wang and X. Jin, *J. Mater. Chem. A*, 2018, **6**, 5555-5559.

7 H. Yang, R. Xu, Y. Yao, S. Ye, X. Zhou and Y. Yu, *Adv. Funct. Mater.*, 2019, **29**, 1809195.

8 Q. Zhang, J. Mao, W. K. Pang, T. Zheng, V. Sencadas, Y. Chen, Y. Liu and Z. Guo, *Adv. Energy Mater.*, 2018, **8**, 1703288.

9 L. Li, H. Jiang, N. Xu, X. Lian, H. Huang, H. Geng and S. Peng, *J. Mater. Chem. A*, 2021, **9**, 17336-17343.

10 Y. Sang, X. Wang, X. Cao, G. F. Ding, Y. H. Ding, Y. N. Hao, N. Xu, H. Z. Yu, L. L. Li and S. J. Peng, *J. Alloys Compd.*, 2020, **831**, 154775.